Impaired Mitochondrial Activity in Insulin Resistant Offspring of Type 2 Diabetics

Rita L. Garcia

YALE UNIVERSITY

Impaired Mitochondrial Activity in Insulin Resistant Offspring of Type 2 Diabetics

A Thesis Submitted to the
Yale University School of Medicine
in Partial Fulfillment of the Requirements for the
Degree of Doctor of Medicine

by
Rina L. Garcia
2004

ABSTRACT

IMPAIRED MITOCHONDRIAL ACTIVITY IN INSULIN RESISTANT OFFSPRING OF TYPE 2 DIABETICS. Rina L. Garcia, Sylvie Dufour, Douglas Befroy, Gerald I. Shulman, and Kitt Falk Petersen. Section of Endocrinology, Department of Internal Medicine, Howard Hughes Medical Institute, Yale University School of Medicine, New Haven, CT.

The current study was undertaken to examine the mechanism of insulin resistance in healthy, young lean insulin resistant offspring of type 2 diabetics compared to age-height-weight-activity matched insulin sensitive control subjects.

Insulin sensitivity of liver and muscle glucose and lipid metabolism were assessed using the euglycemic-hyperinsulinemic clamp, in combination with infusions of [6,6-$^{2}H_{2}$] glucose and [$^{2}H_{5}$]glycerol. ^{1}H magnetic resonance spectroscopy studies were performed to assess intramyocellular lipid and intrahepatic triglyceride content. Local lipolysis was assessed by measuring glycerol release from subcutaneous fat. ^{31}P magnetic resonance spectroscopy was performed *in vivo* to assess rates of ATP synthesis (mitochondrial phosphorylation activity) in the soleus muscle.

Insulin stimulated muscle glucose uptake was approximately 60 percent lower ($P<0.001$ versus control) in the insulin resistant offspring than in the insulin sensitive control subjects and was associated with an approximately 80 percent increase in intramyocellular lipid content ($P=0.005$ versus control). This increase in intramyocellular lipid content is most likely attributable to mitochondrial dysfunction as reflected by an approximately 30 percent reduction in mitochondrial phosphorylation activity ($P=0.01$ versus control) since there were no differences in systemic or localized rates of lipolysis or plasma concentrations of tumor necrosis factor-α, interleukin-6, resistin, or adiponectin.

These data support the hypothesis that insulin resistance in skeletal muscle of insulin resistant offspring is associated with dysregulation of intramyocellular fatty acid metabolism, possibly due to an inherited defect in mitochondrial oxidative-phosphorylation activity.

ACKNOWLEDGEMENTS

Above all, I thank God for the grace and strength He has always given me, especially throughout this project. I would also like to thank William Armando Garcia for being a wonderful husband and for his unconditional support, love and encouragement. Papi, mami y Hillmer gracias por su amor, apoyo y sus sacrificios; sin ellos no hubiera podido lograr estas metas. I am also very grateful to my advisor, Dr. Kitt Falk Petersen, for her excellent professional guidance and mentorship with this project as well as for the personal interest she took in my development as an individual.

I would also like to thank Dr. Mitch Lazar and Michael Lehrke for assistance in measuring plasma resistin concentrations and Yanna Kosover, Mikhail Smolgovsky, Anthony Romanelli, Aida Groszmann, Andrea Belous, Jonas Lai and the staff of the Yale/New Haven Hospital General Clinical Research Center for expert technical assistance with the studies. I would like to especially thank the volunteers for participating in this study.

Lastly, I am grateful to the NIH-NIDDK for the one-year research fellowship that enabled me to participate in this project. This work was supported by grants from the United States Public Health Service: (K23 DK-02347, R01 AG-23686, R01 DK-063192, R01 DK-49230, P30 DK-45735, M01 RR-00125).

TABLE OF CONTENTS

INTRODUCTION

Type 2 diabetes mellitus is reaching epidemic proportions worldwide (1) and in the United States alone there are more than 16 million people living with the disease (2). Although the primary cause of this disease is unknown insulin resistance plays a major role in its development. Insulin resistance is defined as impaired glucose uptake by the muscle. In the progression to diabetes, there is increased glucose production by the liver and an impaired ability of insulin to suppress glucose production. Diabetes develops when there is impaired insulin secretion by the pancreas.

Cross-sectional studies have shown that insulin resistance is present in almost all patients with type 2 diabetes and prospective studies have demonstrated that insulin resistance is the best predictor for an increased risk of developing type 2 diabetes and is often present one to two decades before the onset of the disease (3-5). Furthermore, insulin resistance has been shown to be the best predictor for the later development of the disease (6) in the offspring of parents with type 2 diabetes. In light of this evidence, our focus is to examine the mechanism(s) of insulin resistance in healthy, young, lean individuals whose only confounding risk factor for the development of type 2 diabetes is having (a) type 2 diabetic parent(s).

The factors responsible for insulin resistance are not currently well understood. There is an excellent correlation between plasma non-esterified (free) fatty acid concentrations and insulin sensitivity and more recent studies measuring triglyceride content in muscle biopsies (7) or *in vivo* intramyocellular lipid content by ^{1}H magnetic resonance spectroscopy (MRS) (8-11) have a shown a strong relationship between intramuscular lipid content and insulin resistance in skeletal muscle in insulin resistant

offspring of patients with type 2 diabetes. This suggests that dysregulation of fatty acid metabolism may be responsible for mediating the insulin resistance in these individuals.

In addition, studies have shown that insulin resistance in normoglycemic insulin resistant offspring of type 2 diabetics and in type 2 diabetic subjects is secondary to a defect in insulin-stimulated glucose transport. The postulated mechanism leading to this defect is that increased intramyocellular concentrations of fatty acid metabolites (esp. diacylglycerol, fatty acyl coA) secondary to their increased delivery or decreased intracellular metabolism activate a serine/threonine kinase cascade. This leads to the phosphorylation of serine/threonine sites on insulin receptor substrate-1 and insulin receptor substrate-2, which in turn leads to a decreased ability of these insulin receptor substrates to activate phosphatidylinositol 3-kinase (12-16) (Figure 1). This in turn leads to a decrease in glucose transport activity (17) and a subsequent decrease in glycogen synthesis (18, 19), as well as a decrease in other events occurring downstream of the insulin signaling cascade.

In the current study we examined the mechanism responsible for the accumulation of intramyocellular lipid in young, lean insulin resistant offspring of type 2 diabetic patients. These subjects are ideal for the study of the earliest defects in the pathogenesis of type 2 diabetes as they are young, lean, healthy and are less likely to have any of the confounding factors present in patients with the disease (e.g., hyperglycemia) that can cause insulin resistance *per se*. We hypothesized that intramyocellular lipid accumulation could result from: 1) the increased delivery of lipids from adipocytes secondary to increased basal lipolysis and/or decreased insulin-stimulated suppression of lipolysis and/or 2) decreased rates of mitochondrial oxidative-phosphorylation activity. We

therefore studied these processes in insulin resistant offspring of type 2 diabetic patients and in insulin sensitive control subjects.

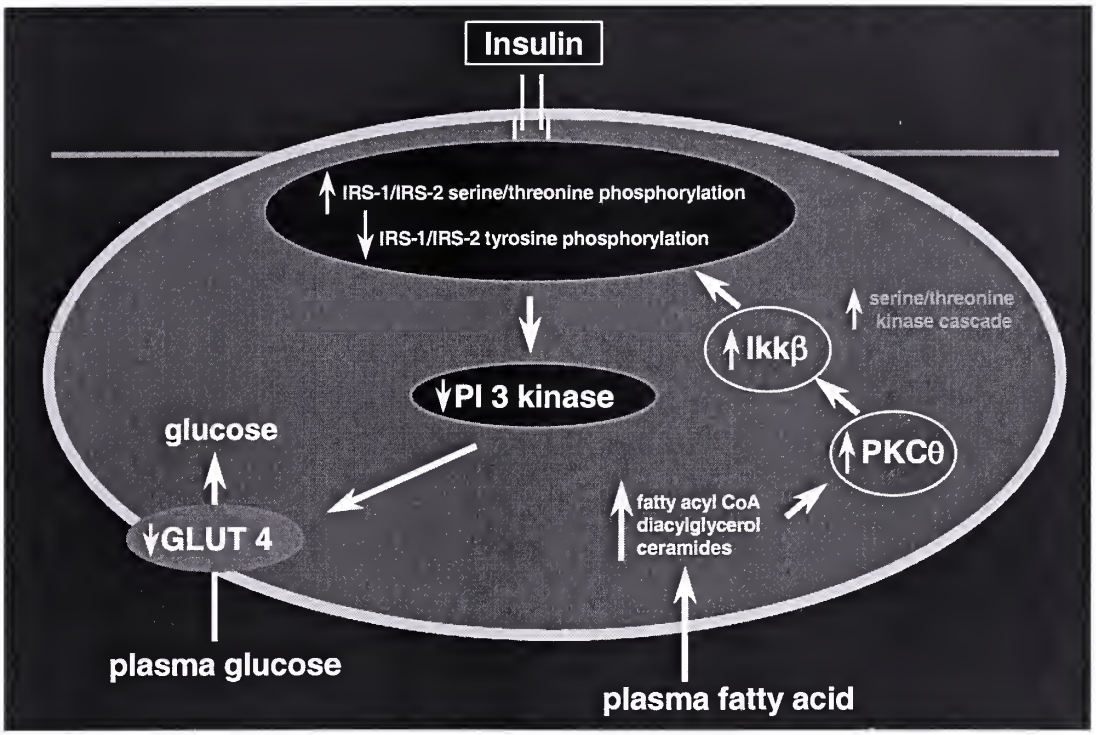

Figure 1. Proposed mechanism of insulin resistance in normoglycemic insulin resistant offspring of type 2 diabetics and in type 2 diabetic subjects. PKCθ, protein kinase Cθ; IRS-1 and IRS-2, insulin receptor substrates; PI 3-kinase, phosphatidylinositol 3-kinase. *Adopted from* (16).

Rates of whole body and subcutaneous fat lipolysis were assessed by measuring rates of whole body [$^2H_5$]glycerol turnover in combination with microdialysis measurements of glycerol release from subcutaneous fat. Rates of *in vivo* mitochondrial phosphorylation activity and the ratio of inorganic phosphate to phosphocreatine (P_i/P_{Cr}) [as an indicator of the relative ratio of type I (mostly oxidative) to type II (mostly glycolytic) muscle fiber types] were assessed in skeletal muscle using ^{31}P MRS. This was done in order to examine whether the ratio of these fibers could account for potential differences in the rates of mitochondrial phosphorylation between the two study groups.

Furthermore, the plasma concentrations of tumor necrosis factor- α (TNF-α), interleukin-6 (IL-6), resistin and adiponectin were measured in the insulin resistant offspring since these adipocyte derived hormones have previously been implicated in causing insulin resistance (20-23).

STATEMENT OF PURPOSE

The overall aim of this study was to examine the mechanism responsible for the accumulation of intramyocellular lipid in young, lean, sedentary, insulin resistant offspring of type 2 diabetic patients. Our first specific aim was to study localized and whole-body lipolysis to examine the hypothesis that intramyocellular lipid accumulation in the insulin resistant offspring results from the increased delivery of lipids from adipocytes secondary to increased basal lipolysis and/or decreased insulin-stimulated suppression of lipolysis. Our second specific aim was to study rates of mitochondrial oxidative phosphorylation in skeletal muscle to examine the hypothesis that intramyocellular lipid content in the insulin resistant offspring results from decreased rates of mitochondrial oxidative-phosphorylation activity.

METHODS

Subjects: All subjects were recruited by local advertising over a two year period and were prescreened to be healthy, 18-46 years old, lean (BMI≤26 kg/m^2), non-smoking and had a birth weight above 5 pounds. All selected subjects were also sedentary, did not exercise regularly and had an Activity Index of less than 3.3, which was calculated using an activity index questionnaire (24). Family history of diabetes was obtained through a family tree that highlighted relatives with type 2 diabetes. The qualifying subjects, approximately 200, were subsequently screened with a standard 75gram [oral glucose load], 3-hour oral glucose tolerance test (OGTT). The subjects were then grouped such that extreme phenotypes for insulin resistance and increased insulin sensitivity were identified. This was determined from the calculation of an Insulin Sensitivity Index (ISI) (25) using the following formula:

$$ISI = \sqrt{\frac{10{,}000}{[(\text{fasting [glucose]} \times \text{fasting [insulin]}) \times (\text{OGTT [glucose]} \times \text{OGTT [insulin]})]}}$$

where [glucose] is expressed in mg/dL, [insulin] is expressed in μU/ml. OGTT [glucose] and OGTT [insulin] are the average plasma glucose and insulin concentrations measured from t=30 to t=180 during the OGTT.

The ISI was used to estimate insulin sensitivity instead of the insulin clamp, the gold standard for assessing insulin sensitivity, because the latter is too labor intensive to be used as a screening tool in large populations. Therefore, data already obtained in the lab comparing ISI and the insulin clamp was used to set ISI cut-off values in order to identify potentially insulin sensitive and insulin resistant individuals.

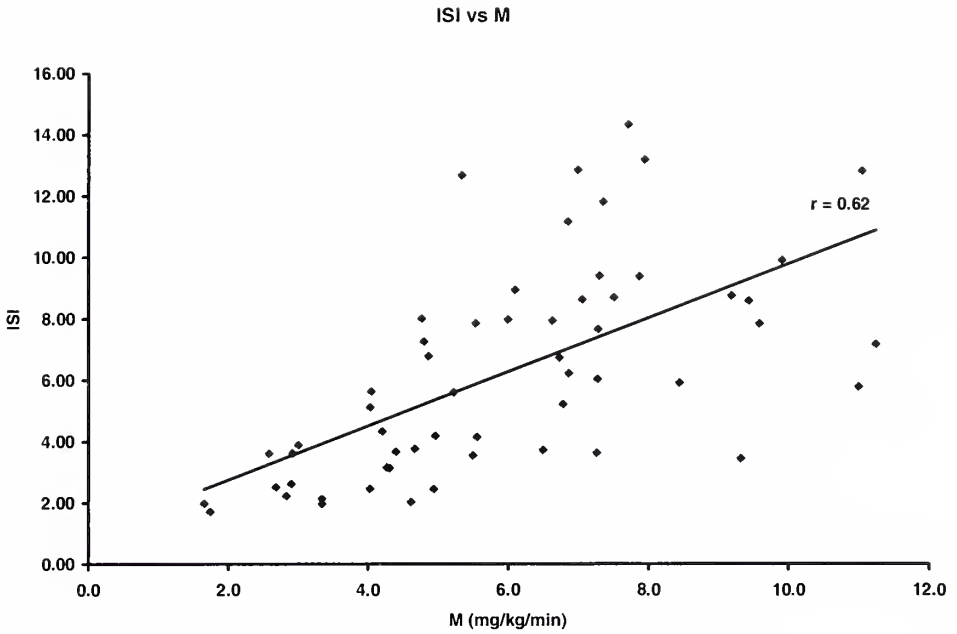

Figure 2. Glucose infusion rate versus insulin sensitivity as assessed by the insulin sensitivity index. ISI, insulin sensitivity index; M, glucose infusion rate.

Furthermore, there was an excellent agreement between the ISI and the M-value obtained during the euglycemic-hyperinsulinemic clamp (r=0.62) (Figure 2). Based on the comparison to the clamp data, insulin resistant offspring (3 males/11 females) were defined to have an insulin sensitivity index of less than 4.0, at least one parent or grandparent with type 2 diabetes and at least one other family member with type 2 diabetes. Insulin sensitive control subjects (5 males/7 females) were defined to have an insulin sensitivity index greater than 6.3 (with or without a family history of type 2 diabetes). All qualifying subjects subsequently underwent a complete medical history and physical examination. In addition, laboratory blood tests were obtained in order to verify normal: blood and platelet count, electrolytes, asparte amino transferase, alanine amino transferase, blood urea nitrogen, creatinine, prothrombin time, partial prothrombin time, cholesterol and triglycerides. Furthermore, subjects were screened for any metal

implants, body piercing and claustrophobia and subsequently underwent ^{1}H MRS studies to assess liver and muscle triglyceride content, as will be described below. After the screening tests, all subjects underwent the euglycemic-hyperinsulinemic clamp study, which is the gold standard for assessing insulin sensitivity of liver, muscle and fat, and/or ^{31}P MRS studies to assess rates of muscle mitochondrial phosphorylation activity. The ^{31}P MRS study also allowed us to evaluate muscle fiber type from P_i/P_{Cr} in the ^{31}P nuclear magnetic resonance spectrum. Two of the twelve control subjects who were initially selected to be insulin sensitive by the ISI from the screening OGTT criteria were subsequently excluded after they were found to be insulin resistant by the euglycemic-hyperinsulinemic clamp. All subjects in the insulin resistant group were also found to be insulin resistant by the insulin clamp. Written consent was obtained from each subject after the purpose, nature and potential complications of the studies were explained. The protocol was approved by the Yale University Human Investigation Committee.

Diet and Study Preparation: Subjects were instructed to consume a regular, weight maintenance diet containing at least 150 g of carbohydrate per day for three days prior to the admission for either the clamp or MRS studies. All subjects were instructed not to perform any exercise other than normal walking for the 3 days prior to the study. The female subjects were studied during the follicular phase of their menstrual cycle (days 0 and 12) in order to minimize changes in ovarian hormonal effects on glucose metabolism (26). Subjects who were taking oral contraceptives were studied irrespective of their menstrual cycle. Subjects were admitted to the Yale-New Haven Hospital General Clinical Research Center the evening before the clamp or ^{31}P MRS study and

remained fasting with free access to regular drinking water until the completion of the study the following day.

Metabolites and Hormones: Plasma glucose concentrations were measured using a YSI STAT 2700 Analyzer (Yellow Springs, CA). Plasma concentrations of insulin, glucagon, adiponectin and resistin were measured using double-antibody radioimmunoassay kits (Linco, St. Louis, MO). Plasma concentrations of TNF-α and IL-6 were measured by Quantine High Sensitivity kits (R&D Systems, Inc., Minneapolis, MN). Plasma fatty acid concentrations were measured using a microfluorometric method (27). Urine nitrogen content was measured at the Mayo Medical Laboratories (Rochester, MN). Microdialysate glycerol concentrations were measured using an enzyme linked colorimetric determination of 0.5 μl samples by a CMA 600 microdialysis analyzer (CMA 600 Microdialysis, N. Chelmsford, MA) (28). Ethanol concentrations were determined enzymatically using a YSI 2700 STAT Analyzer (YSI, Yellow Springs, CA) (28). Gas chromatography mass spectrometer analyses of enrichment of [6,6-$^2H_2$]glucose and [$^2H_5$] glycerol in plasma were performed using a Hewlett-Packard 5971A Mass Selective Detector (Wilimington, DE) (28).

^{1}H Magnetic Resonance Spectroscopic Measurements of Intramyocellular and Intrahepatic Triglyceride Content: On a separate day, all subjects were transported by a wheelchair to the Yale Magnetic Resonance Center. Localized ^{1}H spectra of the soleus muscle were acquired on a 2.1 T Biospec Spectrometer (Bruker Instruments, Inc., Billerica, MA) using a coil assembly consisting of two circular hydrogen-1 coil loops (13 cm diameter each) arranged spatially to generate a quadrature field. During the measurements, the subject remained supine, and the gastrocnemius-

soleus complex of the right leg was positioned within the homogeneous volume of the magnet. Scout images were acquired in order to position the volume of interest. Volumes of interest (15mm x 15mm x 25mm) were centered within the soleus muscle, positioned to avoid vascular structures and gross adipose tissue deposits. Localized shimming in the soleus was performed using FASTERMAP (29) with typical line widths of ~10 Hz obtained. Localized proton spectra were then collected using a PRESS sequence with the following parameters: repetition time (T_R) = 3s; echo time (T_E) = 21.1ms; 8192 data points over 5000 Hz spectral width; 128 scans. Signals in the time domain were multiplied by a Gaussian function prior to Fourier transformation and manual phase correction. ^{1}H resonances were assigned to water and methyl/methylene of triglycerides from their chemical shift, in agreement with Schick et al. (30), and were line fitted using the Mac-Nuts-PPC software package (Acorn NMR, Inc., CA, USA). Intramyocellular lipid (triglyceride) content (IMCL) and extramyocellular lipid content (EMCL) were calculated from the peak areas of intramyocellular CH_2 and extramyocellular CH_2, respectively, with respect to the water peak area, and corrected for T_1 and T_2 relaxation effects. The IMCL and EMCL content were then expressed as a percentage of the muscle water content (28).

Similarly, in order to assess the hepatic lipid content localized ^{1}H NMR spectra of the liver were obtained using a 12 x 14 cm butterfly ^{1}H observation coil placed rigidly over the lateral aspect of the abdomen. Placement of the volume of interest (15mm x 15mm x 15mm) within the liver was ensured by imaging the liver with a multi-slice gradient echo sequence. Prior to each measurement, the H_2O signal was optimized using a shimming procedure, where lipid signal (predominantly from subcutaneous fat) was

suppressed using an inversion recovery method optimized to null the subcutaneous fat signal. Localized proton spectra were collected using a modified PRESS sequence with the following parameters: T_R = 3s; T_E = 24.1ms; 8192 data points over 5000 Hz spectral width; 64 scans. A saturation slice centered on the chest wall was applied to prevent contamination from subcutaneous adipose tissue. The spatial position of the saturation slice was determined for each subject from the scout image. A Lorentzian filter of 5Hz was applied before Fourier transformation and manual phase correction. Hepatic triglyceride content was calculated from the area of intrahepatic CH_2 resonance relative to the area of the water resonance, using the integration routine of Paravision software (Bruker, Billerica, MA), and then expressed as a percentage of liver water content (28).

Euglycemic-Hyperinsulinemic Clamp Procedure: Basal and insulin stimulated rates of glucose and glycerol turnover were assessed during a 3-hour basal period and a 3-hour euglycemic-hyperinsulinemic (20 mU/m2-min) clamp (Figure 3). In order to determine the rates of basal glucose production and glycerol turnover a 3-hour baseline infusion was started at 6 a.m. (t=-180 min) with a primed (3.0 mg/kg) continuous (0.05 mg/kg/min) intravenous infusion of [6,6-$^2H_2$]glucose (99% ^2H enriched) and a continuous infusion of [$^2H_5$]glycerol (0.03 mg/kg/min, 99% ^2H enriched). During the third hour of the baseline infusion a retrograde intravenous catheter was inserted into a hand vein. The hand was warmed in a hot box at 55°C for a sampling of arterialized venous blood, which was collected from this vein at 10-minute intervals during the last 40 minutes of the basal period to measure plasma and insulin concentrations and [6,6-$^2H_2$]glucose and [$^2H_5$]glycerol isotope enrichments. After the blood collection, the basal [6,6-$^2H_2$]glucose infusion was stopped and the euglycemic-hyperinsulinemic clamp was initiated with a

two-step priming dose of insulin (Novolin-R U-100, Novo Nordisk, Princeton, NJ) administered as 80 mU/m^2-min for 5 minutes followed by 40 mU/m^2-min for another 5 minutes. Insulin was then infused at a continuous rate of 20 mU/m^2-min until t=180. The plasma glucose concentrations were increased to and maintained at 100±5 mg/dL with a variable infusion of glucose (20 g/dL of D-20 enriched to approximately 2.5% with [6,6-$^2H_2$]glucose) (31). Plasma glucose concentrations were measured every 5 minutes and the D-20/[6,6-$^2H_2$]glucose infusion was adjusted accordingly. Blood was drawn for measurements of plasma insulin and glucagon concentrations every 30 minutes throughout the clamp. During the last 40 minutes of the clamp period blood was collected for the measurement of plasma glucose and insulin concentrations and [6,6-$^2H_2$]glucose and [$^2H_5$]glycerol isotope enrichments in order to determine the glucose and glycerol turnover rates (28,31).

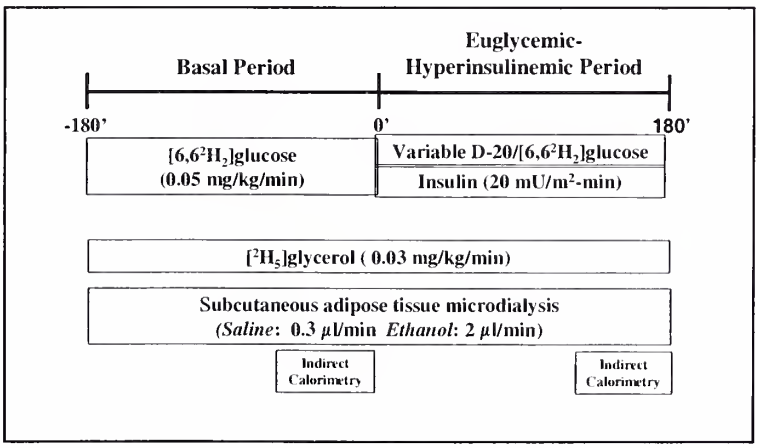

Figure 3. A schematic of the euglycemic-hyperinsulinemic clamp, the "gold standard" technique for the assessment of insulin sensitivity.

Calculations:

Basal glucose production (R_a) was calculated from the infusion rate of the [6,6-$^2H_2$]glucose and the relative enrichments of the [6,6-$^2H_2$]glucose in the infusate (99%) and in the plasma:

R_a= ([6,6-$^2H_2$]glucose infusion rate(mg/min)/body weight (kg)) x([APE_{Inf}/APE_{Plasma}]-1),

where APE_{Inf} is the [6,6-$^2H_2$]glucose infusate Atom Percent Enrichment (99%) and APE_{Plasma} is the baseline steady-state plasma [6,6-$^2H_2$]glucose Atomic Percent Enrichment (%). The term Atomic Percent Enrichment refers to the fraction of isotope of glucose to naturally occurring glucose, expressed as a percentage.

The M-value, the rate of glucose metabolized when plasma glucose concentrations were maintained at 100 mg/dL, was calculated as the mean D-20/[6,6-$^2H_2$]glucose infusion rate over the last 40 minutes of the clamp, corrected for changes in plasma glucose concentrations (32). This correction was calculated using the following formula:

Space Correction = [3.795 x surface area (m^2)/body weight(kg)] x [[$gluc_i$]-[$gluc_f$]],

where [$gluc_i$] and [$gluc_f$] are the initial and final plasma glucose concentrations in mg/dL, respectively, during the 40-minutes time interval in which the M-value was calculated.

The rate of hepatic glucose production during the insulin infusion (R_a) was calculated from the following formula:

$$R_a = M \text{ (mg/kg body weight-min) x } ([APE_{Inf}/APE_{Plasma}]-1),$$

where APE_{Inf} is the exogenous D-20/[6,6-$^2H_2$]glucose infusate Atom Percent Enrichment (which was approximately 2.5%) and APE_{Plasma} is the steady-state clamped plasma [6,6-$^2H_2$]glucose Atom Percent Enrichment (%). To the extent that the plasma [6,6-

$^{2}H_2$]glucose enrichment approximates the [6,6-$^{2}H_2$]glucose enrichment in the D-20/[6,6-$^{2}H_2$]glucose infusate, hepatic glucose production approximates zero and thus a complete suppression of glucose production by insulin is achieved.

The rate of whole body insulin stimulated glucose disposal (R_d) was calculated from the sum of clamped hepatic glucose production (Ra) and the glucose infusion rate (M).

Respiratory exchange measurements: During the last 30 minutes of the baseline period and during the last 30 minutes of the clamp, continuous indirect calorimetry was performed to measure rates of oxygen and carbon dioxide production and of whole body energy expenditure by the ventilated hood technique using the Deltatrack Metabolic Monitor (Sensormedics, Anaheim, CA) (33). These measurements were then used to calculate glucose and fat oxidation using the following formulas:

Glucose oxidation: VO_2 x 0.746 x glucose % of total / body weight (kg)

and

Fat oxidation: VO_2 x 2.029 x fat % of total / body weight (kg),

where VO_2 refers to oxygen consumption in ml/min. The non-protein respiratory quotients for 100% oxidation of fat and for the oxidation of carbohydrates were 0.707 and 1.00, respectively, according to the tables of Lusk (34).

Nonoxidative glucose metabolism, in mg/kg/min, was calculated from the following equation:

Non-oxidative glucose metabolism = M – glucose oxidation,

where M is the glucose metabolism rate in mg/kg/min and glucose oxidation is in mg/kg/min.

Adipose tissue microdialysis: In order to assess *in vivo* rates of localized adipocyte lipolysis two microdialysis probes (CMA/60, CMA, Microdialysis, Solna, Sweden) were inserted into the subcutaneous adipocyte layer on the abdomen, 4-6 cm below the umbilicus (28,35), prior to the initiation of the baseline tracer infusions. Saline was infused through the outer lumen of the first double lumen microdialysis catheter at a rate of 0.3 µl/min, passed through a membrane at the end of the catheter into the adipocyte pad and returned via the inner lumen of the catheter (dialysate). This dialysate was collected in a vial every 30 minutes throughout the baseline and clamp periods. Once steady state was reached, the composition of the dialysate reflected the composition of the interstitial fluid in the adipose pad. Subsequently, the concentration of glycerol was measured in the dialysate (Figure 4).

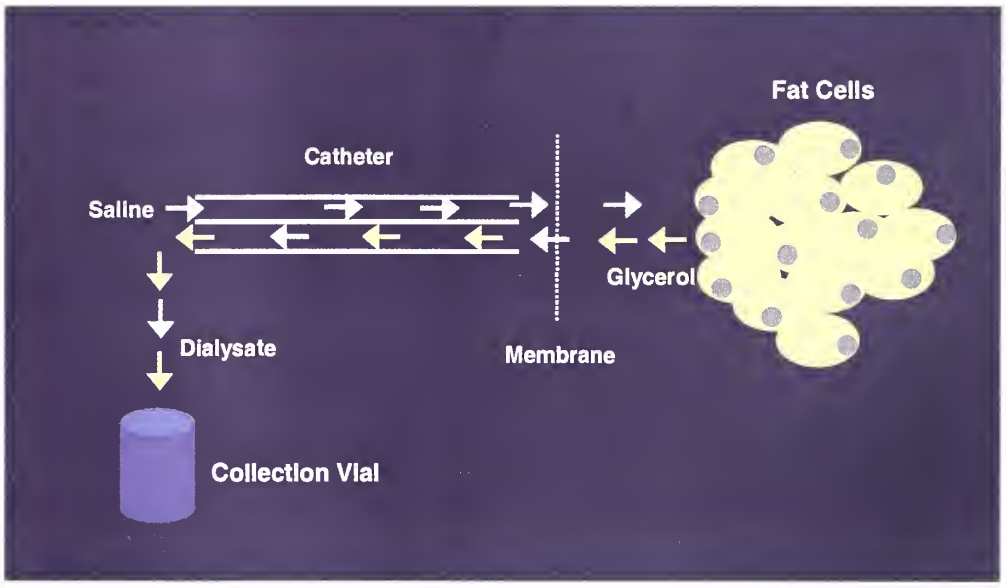

Figure 4. A schematic of the adipocyte microdialysis technique used to measure localized glycerol release from the dialysate collected during the final 30 minutes of the baseline and insulin infusion periods.

The percent suppression of glycerol release from the adipocytes was calculated as the change in the glycerol concentration in the dialysate between the baseline period and the clamp:

$$\text{Percent glycerol suppression} = \frac{Gly_b - Glyc_c}{Gly_b} \times 100\%,$$

where Gly_b represents the basal serum glycerol concentration and Gly_c represents the serum glycerol concentration during the clamp.

Rates of whole-body glycerol turnover (R_a[glyc]) during the basal period and during the clamp was calculated from the following formula:

$$R_a[glyc] = [^2H_5]glyc \text{ infusion rate (mg/min)/body weight (kg)} \times ([APE_{Inf}/APE_{Plasma}]-1),$$

where APE_{Inf} is the $[^2H_5]$glycerol infusate enrichment (99%) and APE_{Plasma} is the steady-state basal plasma $[^2H_5]$glycerol enrichment (%). In order to estimate regional adipose blood flow, an ethanol-based perfusate was infused at a rate of 2 µl/min through the second microdialysis probe. The dialysate was collected, as above, and the ethanol recovery rates were calculated as the ratio of ethanol concentration measured in the perfusate to the ethanol concentration measured in the dialysate.

^{31}P Magnetic Resonance Spectroscopy Measurements of Mitochondrial Phosphorylation Activity and Muscle Fiber Type Composition: Rates of mitochondrial phosphorylation activity were assessed by ^{31}P MRS saturation transfer performed at 36.31 MHz using a flat concentric probe made of a 9-cm diameter inner coil (for ^{31}P) and a 13-cm outer coil tuned to proton frequency for scout imaging and shimming (36). As described above, the scout image was used to guide the position of the volume of interest (~ 1.5 x 2.0 x 6.0 cm^3) within the soleus muscle away from major

vessels, bone and subcutaneous adipose tissue. Unidirectional rates of adenosine triphosphate (ATP) synthesis using the saturation transfer method applied to the exchange between P_i and ATP. The steady state P_i magnetization was measured in the presence of a selective irradiation of the γ resonance of ATP and compared to the equilibrium P_i magnetization in a control spectrum (without irradiation of γ ATP) (36) (Figure 5). That is, the gamma ATP signal in the phosphorous spectrum is saturated and the decrease in P_i is monitored to assess transfer into ATP. Total acquisition time for ^{31}P spectra was about 120 minutes.

P_i/P_{Cr} in the soleus muscle was measured in the same subjects from the spectrum obtained by ^{31}P MRS (37,38), as described above.

Statistical Analyses: Statistical analyses were performed using the Stat View package (Abacus Concepts, Berkeley, CA). To detect statistical differences between control and insulin resistant offspring unpaired student t-tests were performed for independent samples with a P-value (2-sided) of <0.05 considered significant. Non-normally distributed data (i.e. area under the curve data) were log transformed. All data are expressed as means ± SEM.

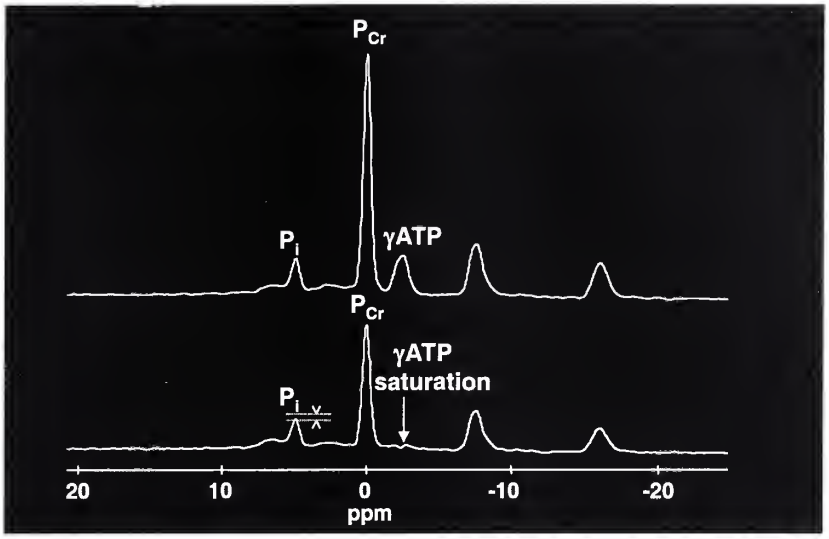

Figure 5. ^{31}P MRS measurement of γATP synthase flux. The top phosphorous spectrum was obtained at equilibrium. During the acquisition of the bottom spectrum, the γATP signal was saturated and the decrease in P_i was monitored to assess its transfer into γATP. ATP, adenosine triphosphate; P_i, inorganic phosphate. P_{Cr}, phosphocreatine. *Adapted from (36).*

Description of Project Involvement: I was involved with subject recruitment and study coordination. I helped in the supervision of most of the OGTTs, calculated the activity index for each subject and performed many of the insulin assays. I also calculated the insulin sensitivity index, which was the basis for the initial allocation of subjects into insulin sensitive control subjects and insulin resistant offspring.

I was present throughout the basal and insulin-stimulated periods of the clamp. During the insulin-stimulated component of the euglycemic-hyperinsulinemic clamp, I administered the stable isotopes [6,6-$^2H_2$]glucose and [$^2H_5$]glycerol at the appropriate infusion rates and calculated and adjusted the D-20/[6,6-$^2H_2$]glucose infusion rate every five minutes. In addition, I changed the microdialysis catheters every 30 minutes, assisted with the collection of blood samples and ensured the comfort of the research subjects.

I performed many of the insulin assays for the euglycemic-hyperinsulinemic clamp and calculated the basal hepatic glucose production rates, rates of insulin-stimulated whole-body glucose disposal and percent suppression of hepatic glucose production. I also calculated the rates of glucose oxidation, non-oxidative glucose metabolism and rates of lipid oxidation from the calorimetry data and calculated the basal and insulin-stimulated whole body glycerol turnover and percent suppression of whole body glycerol release by insulin from the [$^2H_5$] glycerol data. Finally, I calculated the percent suppression of localized lipolysis from the basal and insulin-stimulated glycerol concentrations in the microdialysates.

My advisor, Kitt Falk Petersen, M.D., oversaw all aspects of the study. Sylvie Dufour, Ph.D. and Douglas Befroy, Ph.D. performed the acquisition and the analyses of

the $^{1}H/^{31}P$ magnetic resonance spectroscopic data. Gerald Shulman, M.D., Ph.D. was involved in the overall assessment of the project.

RESULTS

Subject Characteristics: The insulin sensitivity indices for all 200 subjects distributed close to normal, with a slight tendency for a leftward shift (Figure 6).

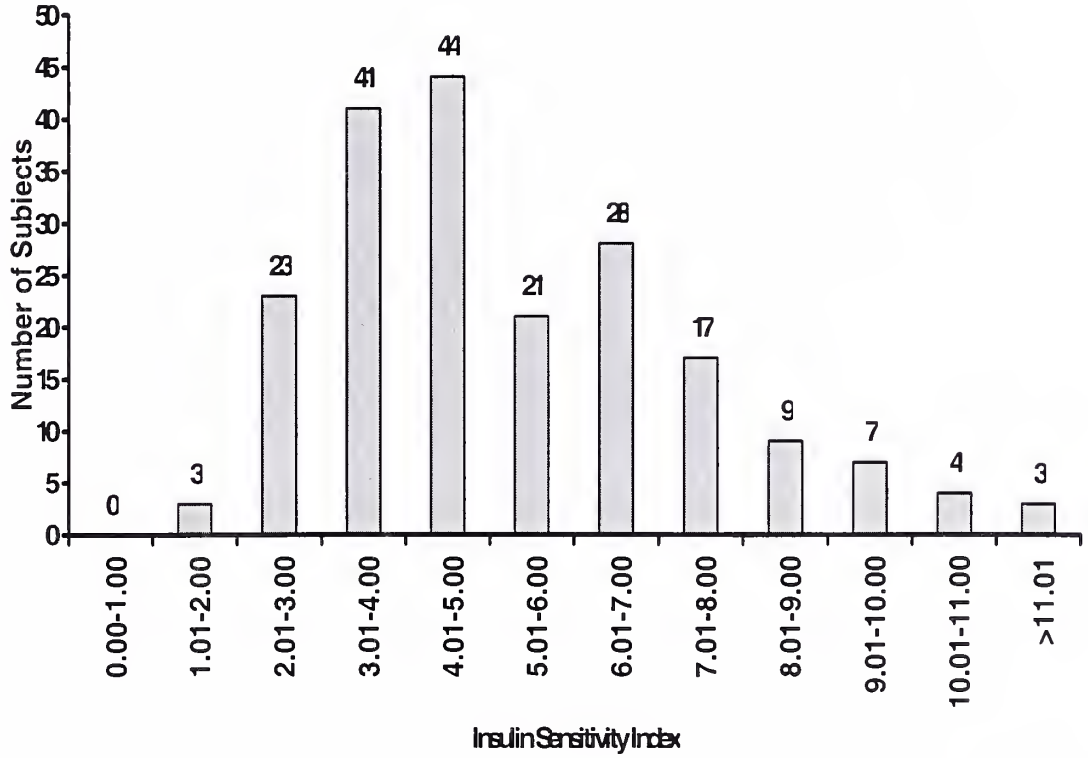

Figure 6. Histogram of the insulin sensitivity index in all subjects who underwent the oral glucose tolerance test; N=200.

Insulin sensitive control and insulin resistant offspring were matched for age, weight, height, body mass index, activity index and had similar basal plasma concentrations of glycosylated hemoglobin, adiponectin, TNF- α, IL-6 and resistin (Table 1). In contrast, the insulin sensitivity index was markedly lower in the insulin resistant offspring (2.8±0.2) compared to the insulin sensitive control subjects (10.2±1.4, $P<0.0001$).

	Insulin Sensitive Controls, N=14	Insulin Resistant Offspring, N=10
Age (years)	28±7	26±7
Weight (kg)	60±13	64±9
Height (m)	1.69±0.11	1.65±0.09
Body Mass Index (kg/m^2)	21±2	23±2
Activity Index	2.6±0.5	2.4±0.4
Glycosylated Hemoglobin (%)	5.1±0.3	5.2±0.4
Adiponectin (μg/ml)	12±4	11±4
TNF-α (pg/ml)	1.5±0.3	1.8±0.9
IL-6 (pg/ml)	0.52±0.31	0.68±0.42
Resistin (ng/ml)	0.77±0.24	0.79±0.24

Table 1. Subject characteristics and fasting plasma concentrations of glycosylatedhemoglobin and adipocyte derived factors in insulin sensitive control and insulin resistant offspring. TNF-α, tumor necrosis factor-α; IL-6, interleukin-6. Data are ± SEM.

Oral Glucose Tolerance Test: All subjects had normal glucose tolerance (fasting plasma glucose < 110 mg/dL, 2-hour postload glucose <140 mg/dL), as determined by the OGTT, but the plasma glucose (Figure 7a) and insulin (Figure 7b) concentrations before and during the test were significantly higher in the insulin resistant offspring. Basal plasma fatty acid concentrations were similar in the insulin sensitive control (0.37±0.05 mM) and insulin resistant offspring (0.47±0.05 mM, P=0.17) and decreased by approximately 80% in both groups during the glucose tolerance test (Figure 7c). There were no differences in the basal plasma glucagon concentrations in the insulin sensitive control (56±4 pg/ml) and insulin resistant offspring (59±3 pg/ml, P=0.64).

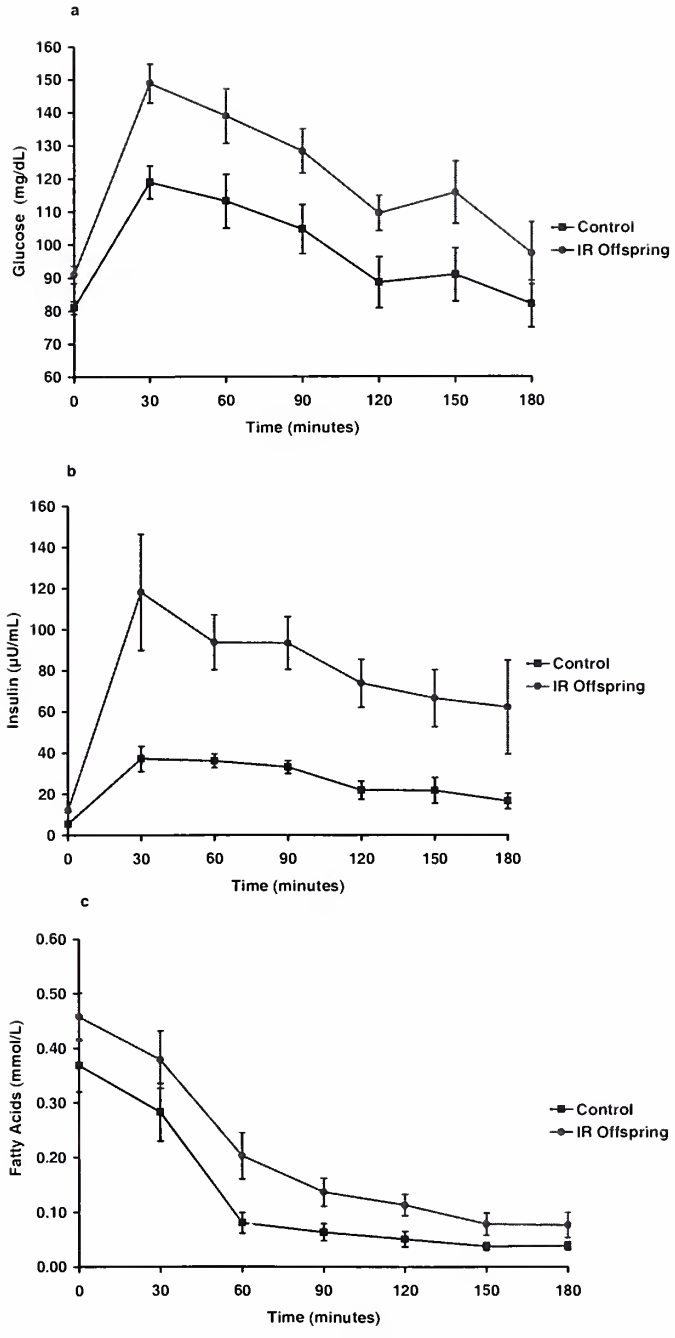

Figure 7. Plasma concentrations of: (a) glucose*, (b) insulin† (c) free fatty acids before and during an oral glucose tolerance test in insulin sensitive control (n=9) and insulin resistant offspring (n=14). (P=0.016 for area under the curve for glucose concentration between insulin sensitive controls and insulin resistant offspring; P=0.002 for area under the curve for insulin concentration between control and insulin resistant offspring). *To convert glucose values to millimole per liter, divide by 18, †To convert insulin values to pmole per liter multiply by 6.0.

Euglycemic-Hyperinsulinemic Clamps: Basal rates of glucose production were similar in the insulin sensitive control subjects (2.3±0.1 mg/kg/min, N=9) and insulin resistant offspring subjects (2.0±0.3 mg/kg/min, N=8, p=0.41) and suppressed completely in both groups during the euglycemic-hyperinsulinemic clamp. In contrast, rates of glucose infusion required to maintain euglycemia (control: 7.7±0.5 mg/kg/min and insulin resistant offspring: 3.3±0.3 mg/kg/min, P<0.001) and insulin stimulated rates of peripheral glucose uptake were approximately 60% lower in the insulin resistant offspring subjects compared to the insulin sensitive control subjects during the clamp (Figure 8). This reduction in peripheral glucose metabolism could mostly be attributed to an approximately 70% reduction (P<0.001) in nonoxidative glucose disposal in the insulin resistant offspring (Figure 8).

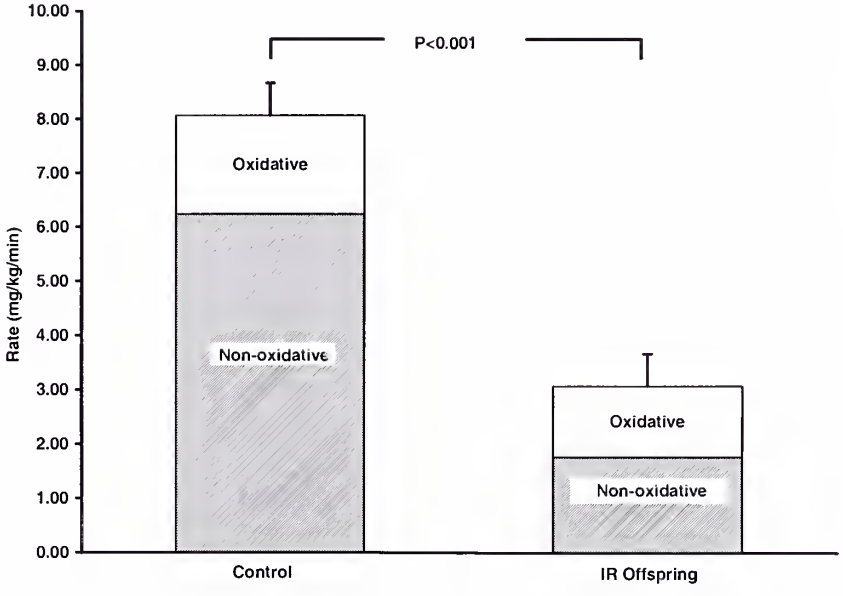

Figure 8. Rates of insulin stimulated glucose metabolism were lower in the insulin resistant (IR) offspring (N=8), which could be attributed to an approximately 70% reduction in non-oxidative glucose disposal in this group, compared to insulin sensitive control subjects (N=9).

There were no differences between the two groups in basal or insulin stimulated rates of: *glucose oxidation* [(Basal; control: 0.8±0.2 mg/kg/min, insulin resistant offspring: 0.9±0.2 mg/kg/min, P=0.76), (Insulin Stimulated; control: 1.8.±0.2 mg/kg/min, insulin resistant offspring: 1.3±0.2 mg/kg/min, P=0.12)], *rates of whole body lipid oxidation* [(Basal; control: 4.2±0.9 mg/kg/min, insulin resistant offspring: 3.0±0.6 mg/kg/min, P=0.32), (Insulin Stimulated; control: 1.3±0.5 mg/kg/min, insulin resistant offspring: 2.0±0.6 mg/kg/min, P=0.36)], or *respiratory quotient (rates of oxygen uptake/rates of carbon dioxide production, in ml/min)* [(Basal; control: 0.81±0.02, insulin resistant offspring: 0.82±0.02, P=0.80), (Insulin Stimulated; control: 0.91±0.02, insulin resistant offspring: 0.87±0.02, P=0.21). Basal (control: 24.6±1.1 kcal/kg/24h, insulin resistant offspring: 21.8±0.7 kcal/kg/24h, P=0.06) and insulin stimulated (control: 24.9±0.7 kcal/kg/24h, insulin resistant offspring: 21.6±0.9 kcal/kg/24h, P=0.01) rates of whole body energy expenditure tended to be lower in the insulin resistant offspring.

Whole Body and Localized Rates of Glycerol Metabolism: Basal rates of whole body glycerol turnover (control: 0.21±0.03 μmol/min, insulin resistant offspring: 0.18±0.02 μmol/min, P=0.32) and insulin suppression of glycerol turnover during the clamp (control: 0.11±0.01 μmol/min, insulin resistant offspring: 0.09±0.01 μmol/min, P=0.32) were similar in the control and insulin resistant offspring (Figure 9).

Consistent with this finding the interstitial glycerol concentrations, assessed by microdialysis, decreased by a similar degree in the insulin sensitive control subjects (36±7%) and insulin resistant offspring (41±6%, P=0.67) during the euglycemic-hyperinsulinemic clamp (Figure 10).

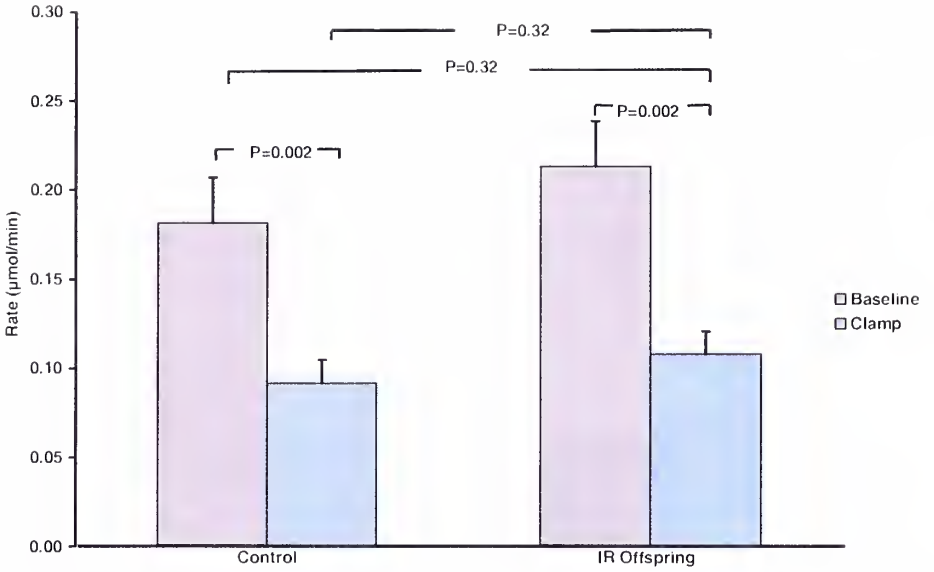

Figure 9. Rates of whole body glycerol turnover were not significantly different between the insulin resistant (IR) offspring and insulin sensitive control subjects at baseline and suppressed comparably during the insulin infusion.

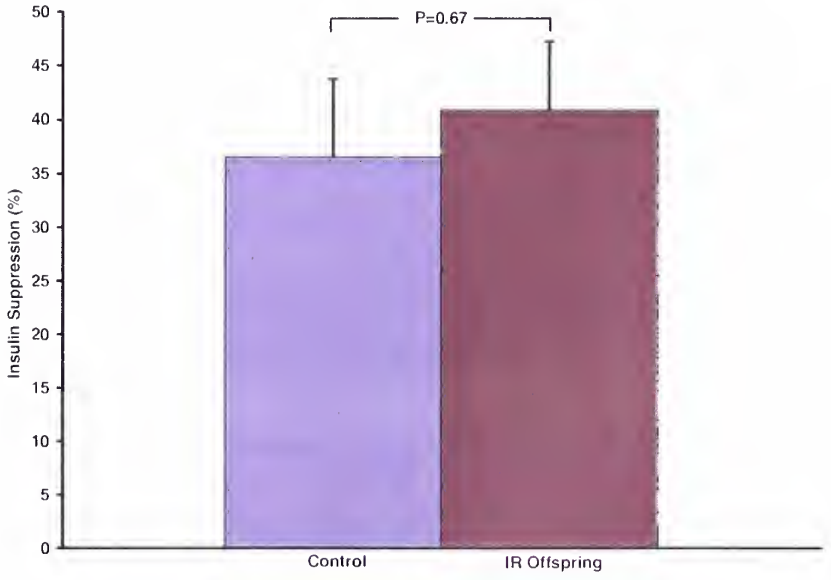

Figure 10. There was no significant difference in the ability of insulin to suppress local glycerol release from adipocytes, as measured by microdialysis, between the insulin resistant (IR) offspring and insulin sensitive control subjects.

^{1}H Magnetic Resonance Spectroscopy assessment of Intramyocellular and Intrahepatic Triglyceride Content: The intramyocellular lipid content in the soleus muscle, as determined by ^{1}H MRS, was increased by approximately 80% (P=0.005) in the insulin resistant offspring (N=12) compared to the insulin sensitive control subjects (N=10) (Figure 11).

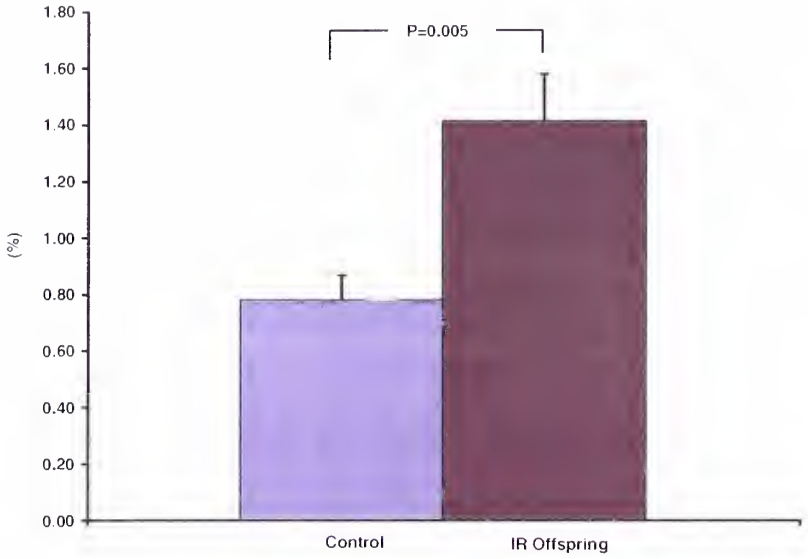

Figure 11. Intramyocellular lipid content was approximately 80% higher in the insulin resistant offspring, as compared to the control subjects.

There was a tendency, although not significant, for the intrahepatic triglyceride content to be higher in the insulin resistant offspring (2.35±1.49 percent) compared to the insulin sensitive control subjects (0.47±0.16 percent, P=0.29).

^{31}P Magnetic Resonance Spectroscopy Assessment of Mitochondrial Phosphorylation Activity and Muscle Fiber Type Composition: Rates of mitochondrial phosphorylation activity in skeletal muscle were approximately 30 percent lower (P=0.01) in the insulin resistant offspring (N=13) compared to the insulin sensitive control subjects (N=10) (Figure 12).

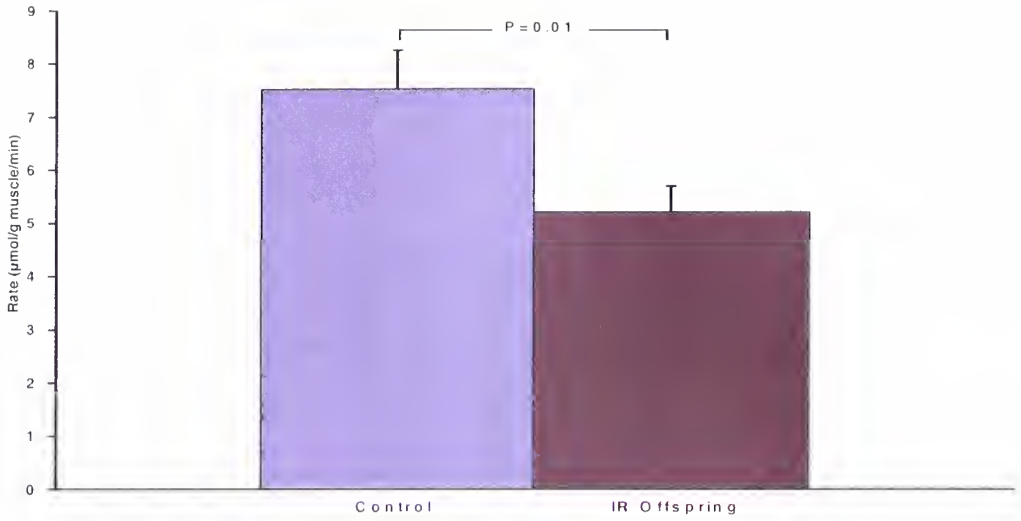

Figure 12. Rates of muscle mitochondrial phosphorylation activity in skeletal muscle of were approximately 30% lower in insulin resistant (IR) offspring, as compared to insulin sensitive control subjects.

The ratio of type I/type II fiber type composition of the soleus muscle, as reflected by P_I/P_{CI}, was reduced by approximately 20 percent (P=0.002) in the insulin resistant offspring (0.113±0.004) compared to the insulin sensitive control subjects (0.137±0.005).

DISCUSSION

In this study, we examined the mechanism of insulin resistance in lean insulin resistant offspring of type 2 diabetic patients, compared to age-height-weight-activity matched insulin sensitive control subjects. Specifically, we examined two possible hypotheses that could account for the accumulation of intramyocellular lipids and thus insulin resistance in our study population: 1) increased fatty acid delivery to the muscle cells secondary to defects in lipolysis and 2) decreased fatty acid oxidation secondary to defects in mitochondrial oxidative-phosphorylation activity in the muscle.

As expected, we found that the insulin resistant offspring were severely insulin resistant, compared to the insulin sensitive control subjects, and that this could mostly be attributed to an approximately 70 percent reduction in insulin stimulated non-oxidative muscle glucose metabolism. As expected, using ^{1}H MRS to measure intramyocellular lipid content we found that insulin resistance in muscle was accompanied by an approximately 80 percent increase in intramyocellular lipid content in the insulin resistant offspring compared to insulin sensitive control subjects. These data are consistent with previous studies in man (8-10) and rodents (39, 40) that have suggested an important role of dysregulated intramuscular fatty acid metabolism in causing insulin resistance and supports a similar role for fat induced insulin resistance in skeletal muscle of insulin resistant offspring.

In order to examine whether the increase in intramyocellular lipid content in the insulin resistant offspring was due to increased delivery of fatty acids to the muscle we measured whole body and localized rates of lipolysis. Rates of whole body lipolysis were similar in the control and insulin resistant offspring during the basal state and suppressed

equally during the euglycemic-hyperinsulinemic clamp. Consistent with this finding we found that insulin suppression of localized rates of lipolysis in subcutaneous fat, assessed by microdialysis, was also similar in both groups. Taken together these data suggest that insulin resistance was confined mostly to skeletal muscle and that increased basal rates of peripheral lipolysis, and/or defects in insulin suppression of lipolysis, do not play a major role in causing the increased intramyocellular lipid content observed in the insulin resistant offspring.

In order to assess whether decreased mitochondrial activity might be a contributing factor to the increased intramyocellular lipid content we also assessed rates of muscle mitochondrial phosphorylation activity *in vivo* by ^{31}P MRS. Using this procedure we found that rates of mitochondrial ATP production were reduced by approximately 30 percent in muscle of the insulin resistant offspring compared to the insulin sensitive control subjects. One possible explanation for this finding might be a lower ratio of type I fibers (mostly oxidative) to type II fibers (mostly glycolytic) in the insulin resistant offspring. In order to test this possibility we also performed ^{31}P MRS measurements to noninvasively assess the relative P_i/P_{Cr}, which has been shown to be an excellent indicator of the relative ratio of type I to type II muscle fibers (37, 38), and found that the insulin resistant offspring had a approximately 20 percent reduction in the ratio of type I to type II muscle fiber types. This finding is consistent with a biopsy study by Nyholm et al. in which an increased number of type IIb muscle fibers was found in overweight insulin resistant first degree relatives of patients with type 2 diabetes (41). Taken together these data suggest that insulin resistant offspring have an inherited

reduction in mitochondrial content in muscle, which in turn may be responsible for the reduced rates of mitochondrial oxidative-phosphorylation activity.

Several recent studies have also implicated several novel adipocyte derived factors in mediating insulin resistance in obesity and type 2 diabetes (20, 21, 41-45). In order to address the potential role of resistin, TNF-α, IL-6 and adiponectin in mediating insulin resistance in the insulin resistant offspring we measured the plasma concentrations of these factors and found no differences between the two groups. These data suggest that alterations in plasma concentrations of these adipocyte-derived factors do not have a major role in mediating insulin resistance in insulin resistant offspring.

In summary, to our knowledge, these are the first studies to assess systemic and localized rates of lipolysis, adipocyte derived factors, mitochondrial phosphorylation activity and fiber type in muscle of healthy young, lean, normoglycemic insulin resistant offspring. Taken together these results support the hypothesis that insulin resistance in the insulin resistant offspring is due to dysregulation of intramyocellular fatty acid metabolism which may be caused by an inherited defect in mitochondrial oxidative-phosphorylation activity, which in turn may be attributed to a reduced ratio of type I/type II muscle fiber types. These results are similar to those observed in insulin resistant lean elderly subjects which, in contrast, are likely attributable to acquired defects in mitochondrial biogenesis leading to reduced skeletal muscle mitochondrial content (46) (Figure 13). Furthermore since mitochondria play a critical role in mediating glucose induced insulin secretion (47) similar inherited defects in beta cell mitochondrial function/content, in the setting of peripheral insulin resistance, might explain the very high incidence of diabetes in these individuals (6).

In this regard it is of interest that a common Gly482Ser polymorphism of peroxisome proliferator-activated receptor γ coactivator-1, a transcriptional regulator of genes responsible for mitochondrial biogenesis and fat oxidation (48), has been linked to an increased relative risk for type 2 diabetes in Danish (49) populations as well as altered lipid oxidation and insulin secretion in Pima Indians (50). These data also identify mitochondrial oxidative-phosphorylation activity as a potential novel therapeutic target for prevention and treatment of type 2 diabetes. Additionally, two very recent DNA microarray analysis studies suggest that a coordinated reduction of PGC-1α genes involved in oxidative phosphorylation occurs in skeletal muscle of overweight patients with type 2 diabetes (51) and in obese Mexican-Americans with type 2 diabetes and overweight family history-positive non-diabetic subjects (52).

Future studies in our laboratory will address the question of whether a decrease in intramyocellular lipid content through a small weight loss will lead to an improvement in insulin sensitivity in normal weight insulin resistant offspring of type 2 diabetics. Another study will examine the number of mitochondria in the muscle of these offspring to assess whether a decrease in mitochondrial number could account for the decreased activity in mitochondrial oxidative-phosphorylation that was observed in the current study.

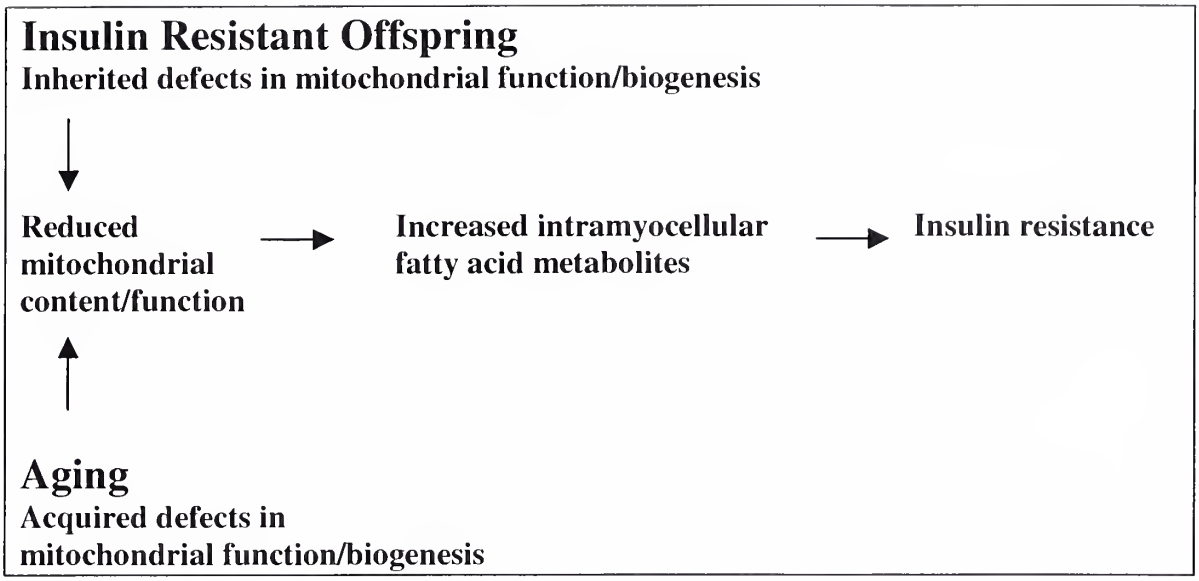

Figure 13. Proposed mechanism for the development of insulin resistance in insulin resistant offspring of type 2 diabetics and the elderly.

REFERENCES

1. Zimmet P, Alberti KG, Shaw J. 2001. Global and societal implications of the diabetes epidemic. Nature. 414:782-7.

2. American Diabetes Association. 2000. Report of the expert committee on the diagnosis and classification of diabetes mellitus. Diabetes Care. Clinical Practice Recommendations. 23 (suppl 1):S4-S19.

3. Lillioja S, Mott DM, Howard BV, Bennet PH, Yki-Jarvinen H., et al. 1988. Impaired glucose tolerance as a disorder of insulin action. Longitudinal and cross-sectional studies in Pima Indians. N Engl J Med. 318:1217-25.

4. Lillioja S, Mott DM, Spraul M, Ferraro R, Foley JE, et al. 1993. Insulin resistance and insulin secretory dysfunction as precursors of non-insulin-dependent diabetes mellitus. Prospective studies of Pima Indians. N Engl J Med. 329:1988-92.

5. DeFronzo RA, Bonadonna RC, Ferrannini E. 1992. Pathogenesis of NIDDM. A balanced overview. Diabetes.Care. 15:318-368.

6. Warram JH, Martin BC, Krolewski AS, Soeldner JS, Kahn CR. 1990. Slow glucose removal rate and hyperinsulinemia precede the development of type II diabetes in the offspring of diabetic parents. Ann Intern Med. 113:909-15.

7. Johnson AB, Argyraki M, Thow JC, Cooper BG, Fulcher G, Taylor R. 1992. Effect of increased free fatty acid supply on glucose metabolism and skeletal muscle glycogen synthase activity in normal man. Clin Sci (Lond). 82:219-26.

8. Krssak M, Falk Petersen K, Dresner A, DiPietro L, Vogel SM, et al. 1999. Intramyocellular lipid concentrations are correlated with insulin sensitivity in humans: a ^{1}H NMR spectroscopy study. Diabetologia. 42:113-6.

9. Perseghin G, Scifo P, De Cobelli F, Pagliato E, Battezzati A, et al. 1999. Intramyocellular triglyceride content is a determinant of in vivo insulin resistance in humans: a 1H-13C nuclear magnetic resonance spectroscopy assessment in offspring of type 2 diabetic parents. Diabetes. 48:1600-6.

10. Szczepaniak LS, Babcock EE, Schick F, Dobbins RL, Garg A, et al. 1999. Measurement of intracellular triglyceride stores by H spectroscopy: validation in vivo. Am J Physiol. 276:E977-89.

11. Perseghin G, Ghosh S, Gerow K, Shulman GI. 1997. Metabolic defects in lean nondiabetic offspring of NIDDM parents: a cross-sectional study. Diabetes. 46:1001-9.

12. Griffin ME, Marcucci MJ, Cline GW, Bell K, Barucci N, et al. 1999. Free fatty acid-induced insulin resistance is associated with activation of protein kinase C theta and alterations in the insulin signaling cascade. Diabetes. 48:1270-4.

13. Dresner A, Laurent D, Marcucci M, Griffin ME, Dufour S, et al. 1999. Effect of free fatty acids on glucose transport and IRS-1-associated phosphatidylinositol 3-kinase activity. J Clin Invest. 103:253-259.

14. Yu C, Chen Y, Cline GW, Zhang D, Zong H, et al. 2002. Mechanism by which fatty acids inhibit insulin activation of insulin receptor substrate-1 (IRS-1)-associated phosphatidylinositol 3-kinase activity in muscle. J Biol Chem. 277:50230-6.

15. Itani SI, Ruderman NB, Schmieder F, Boden G. 2002. Lipid-induced insulin resistance in human muscle is associated with changes in diacylglycerol, protein kinase C, and IkappaB-alpha. Diabetes. 51:2005-11.

16. Shulman GI. 2000. Cellular mechanisms of insulin resistance. J Clin Invest. 106(2): 171-6.

17. Dresner A, Laurent D, Marcucci M, Griffin ME, Dufour S, et al. 1999. Effects of free fatty acids on glucose transport and IRS-1-associated phosphatidylinositol 3-kinase activity. J Clin Invest. 103:253-9.

18. Boden G, Chen X, Ruiz J, White JV, Rossetti L 1994. Mechanisms of fatty acid-induced inhibition of glucose uptake. J Clin Invest. 93:2438-46.

19. Roden M, Price TB, Perseghin G, Petersen KF, Rothman DL, et al. 1996. Mechanism of free fatty acid-induced insulin resistance in humans. J Clin Invest. 97:2859-65.

20. Hotamisligil GS, Shargill NS, Spiegelman BM. 1993. Adipose expression of TNF-α: direct role in obesity-linked insulin resistance. Science. 259:87-91.

21. Kern PA, Ranganathan S, Li C, Wood L, Ranganathan G. 2001. Adipose tissue TNF and IL-6 expression in human obesity and insulin resistance. Am J Physiol Endocrinol Metab. 280:E745-51.

22. Steppan CM, Bailey ST, Bhat S, Brown EJ, Banerjee RR et al. 2001. The hormone resistin links obesity to diabetes. Nature. 409:307-12.

23. Yamauchi T, Kamon J, Waki H, Terauchi Y, Kubota N, et al. 2001. The fat-derived hormone adiponectin reverses insulin resistance associated with both lipoatrophy and obesity. Nat Med. 7:941-6.

24. Baecke JA, Burema J, Frijters JE. 1982. A short questionnaire for the measurement of habitual physical activity in epidemiological studies. Am J Clin Nutr. 36:936-42.

25. Matsuda M, DeFronzo RA. 1999. Insulin sensitivity indices obtained from oral glucose tolerance testing: comparison with the euglycemic insulin clamp. Diabetes Care. 22:1462-70.

26. Diamond MP, Jacob R, Connolly-Diamond M, DeFronzo RA. 1993. Glucose metabolism during the menstrual cycle. Assessment with the euglycemic, hyperinsulinemic clamp. J Reprod Med. 38:417-21.

27. Miles J, Glasscock R, Aikens J, Gerich J, Haymond M. 1983. A microfluorometric method for the determination of free fatty acids in plasma. J Lipid Res. 24:96-9.

28. Mayerson AB, Hundal RS, Dufour S, Lebon V, Befroy D et al. 2002. The effects of rosiglitazone on insulin sensitivity, lipolysis, and hepatic and skeletal muscle triglyceride content in patients with type 2 diabetes. Diabetes. 51:797-802.

29. Shen J, Rycyna RE, Rothman DL. 1997. Improvements on an in vivo automatic shimming method [FASTERMAP]. Magn Reson Med. 38:834-839.

30. Schick F, Eismann B, Jung WI, Bongers H, Bunse M, Lutz O. 1993. Comparison of localized proton NMR signals of skeletal muscle and fat tissue in vivo: two lipid compartments in muscle tissue. Magn Reson Med. 29:158-167.

31. Maggs DG, Buchanan TA, Burant CF, Cline G, Gumbiner B, et al. 1998. Metabolic effects of troglitazone monotherapy in type 2 diabetes mellitus. A randomized, double-blind, placebo-controlled trial. Ann Intern Med. 128:176-85.

32. DeFronzo RA, Tobin JD, Andres R. 1979. Glucose clamp technique: a method for quantifying insulin secretion and resistance. Am J Physiol. 237(3):E214-23 Sep.

33. Petersen KF, Hendler R, Price T, Perseghin G, Rothman DL, et al. 1998. 13C/31P NMR studies on the mechanism of insulin resistance in obesity. Diabetes. 47:381-6.

34. Lusk G. 1924. Animal calorimetry: analysis of the oxidation of mixtures of carbohydrates and fat. A correction. J Biol Chem. 59:41-42.

35. Lafontan M, Arner P. 1996. Application of *in situ* microdialysis to measure metabolic and vascular responses in adipose tissue. Trends Pharmacol Sci. 17:309-313.

36. Lebon V, Dufour S, Petersen KF, Ren J, Jucker BM, et al. 2001. Effect of triiodothyronine on mitochondrial energy coupling in human skeletal muscle. J Clin Invest. 108:733-7.

37. Meyer RA, Brown TR, Kushmerick MJ. 1985. Phosphorus nuclear magnetic resonance of fast and slow-twitch muscle. Am J Physiol. 248:C279-87.

38. Vandenborne K, Walter G, Ploutz-Snyder L, Staron R, Fry A, et al. 1995. Energy-rich phosphates in slow and fast human skeletal muscle. Am J Physiol. 268:C869-76.

39. Kraegen EW, Clark PW, Jenkins AB, Daley EA, Chisholm DJ, Storlien LH. 1991. Development of muscle insulin resistance after liver insulin resistance in high-fat-fed rats. Diabetes. 40:1397-403.

40. Kim JK, Fillmore JJ, Chen Y, Yu C, Moore IK, et al. 2001. Tissue-specific overexpression of lipoprotein lipase causes tissue-specific insulin resistance. Proc Natl Acad Sci U S A. 98:7522-7.

41. Nyholm B, Qu Z, Kaal A, Pedersen SB, Gravholt CH, et al. 1997. Evidence of an increased number of type IIb muscle fibers in insulin-resistant first-degree relatives of patients with NIDDM. Diabetes. 46:1822-8.

42. Steppan CM, Lazar MA. 2002. Resistin and obesity-associated insulin resistance. Trends Endocrinol Metab. 13:18-23.

43. Tsao TS, Lodish HF, Fruebis J. 2002. ACRP30, a new hormone controlling fat and glucose metabolism. Eur J Pharmacol. 440:213-21.

44. Pajvani UB, Scherer PE. Adiponectin: systemic contributor to insulin sensitivity. 2003. Curr Diab Rep. 3:207-13.

45. Yamauchi T, Kamon J, Minokoshi Y, Ito Y, Waki H, et al. 2002. Adiponectin stimulates glucose utilization and fatty-acid oxidation by activating AMP-activated protein kinase. Nat Med. 8:1288-95.

46. Petersen KF, Befroy D, Dufour S, Dziura J, Ariyan C, et al. 2003. Mitochondrial dysfunction in the elderly: possible role in insulin resistance. Science. 300:1140-2.

47. Luft R, Luthman H. [Physiopathology of mitochondria. 1993. From Luft's disease to aging and diabetes]. Lakartidningen. 90:2770-5.

48. Wu Z, Puigserver P, Andersson U, Zhang C, Adelmant G, et al. 1999. Mechanisms controlling mitochondrial biogenesis and respiration through the thermogenic coactivator PGC-1. Cell. 98:115-24.

49. Ek J, Andersen G, Urhammer SA, Gaede PH, Drivsholm T, et al. 2001. Mutation analysis of peroxisome proliferator-activated receptor-gamma coactivator-1 (PGC-1) and relationships of identified amino acid polymorphisms to Type II diabetes mellitus. Diabetologia. 44:2220-6.

50. Muller YL, Bogardus C, Pedersen O, Baier LA. 2003. Gly482Ser missense mutation in the peroxisome proliferator-activated receptor gamma coactivator-1 is associated with altered lipid oxidation and early insulin secretion in Pima Indians. Diabetes. 52:895-8.

51. Mootha VK, Lindgren CM, Eriksson KF, Subramanian A, Sihag S, et al. 2003. PGC-1alpha-responsive genes involved in oxidative phosphorylation are coordinately downregulated in human diabetes. Nat Genet. 34:267-73.

52. Patti ME, Butte AJ, Crunkhorn S, Cusi K, Berria R, et al. 2003. Coordinated reduction of oxidative metabolism in humans with insulin resistance and diabetes: Potential role of PGC1 and NRF1. Proc Natl Acad Sci USA. 100:8466-71.

HARVEY CUSHING/JOHN HAY WHITNEY MEDICAL LIBRARY

MANUSCRIPT THESES

Unpublished theses submitted for the Master's and Doctor's degrees and deposited in the Medical Library are to be used only with due regard to the rights of the authors. Bibliographical references may be noted, but passages must not be copied without permission of the authors, and without proper credit being given in subsequent written or published work.

This thesis by
has been used by the following person, whose signatures attest their acceptance of the above restrictions.

NAME AND ADDRESS **DATE**